

## Impact of gas bubbles on bacterial adhesion on super-hydrophobic aluminum surfaces

Md Elius<sup>a</sup>, Stephanie Richard<sup>b</sup>, Kenneth Boyle<sup>b</sup>, Wei-Shun Chang<sup>c</sup>, Pia H. Moisander<sup>b</sup>, Hangjian Ling<sup>a,\*</sup>

<sup>a</sup> Department of Mechanical Engineering, University of Massachusetts Dartmouth, Dartmouth, MA 02747, USA

<sup>b</sup> Department of Biology, University of Massachusetts Dartmouth, Dartmouth, MA 02747, USA

<sup>c</sup> Department of Chemistry & Biochemistry, University of Massachusetts Dartmouth, Dartmouth, MA 02747, USA



### ARTICLE INFO

#### Keywords:

Super-hydrophobic surface  
Micro/nano-scale gas bubbles  
Bacterial adhesion  
Anti-biofouling

### ABSTRACT

Super-hydrophobic surface (SHS), which traps micro/nano-scale gas bubbles on solid walls, has been reported to greatly reduce bacterial adhesion and biofouling. However, it is unclear whether and how the trapped gas bubbles reduce the bacterial adhesion. Here, we examine the role of the trapped gas on the bacterial adhesion by measuring the spatial distributions of attached bacteria on SHS using scanning electron microscopy (SEM). Two SHSs, one with regular micro-grooves, and the other with randomly roughed textures at micro/nano-scales, both created on aluminum substrates, were tested. We found that for a SHS where gas bubbles are trapped between roughness elements, bacteria only attach to the surface areas that are not covered by gas (e.g., top of roughness elements), while the areas covered by gas bubbles - gaps between roughness elements - are free of bacteria. In contrast, for a rough surface with the same texture geometry as that of SHS but no hydrophobic chemistry, bacteria are distributed evenly to the top and gap of roughness elements. Our results suggest that the SHS may reduce biofouling by providing a physical barrier of gas-liquid interface which separates bacteria from the solid walls. Furthermore, we showed that nano-scale roughness on SHS is insufficient to prevent bacterial adhesion. Our results should provide useful guidance for the future engineering design of efficient anti-biofouling materials.

### 1. Introduction

Biofilms, which are surface-attached bacterial communities embedded in a self-produced extracellular matrix (Costerton et al., 1995), are known to produce adverse impacts such as marine biofouling (Callow and Callow, 2002; Fitridge et al., 2012), persistence of pathogens (Habash and Reid, 1999; Mihai, 2015) and food contamination (Myszka and Czaczyk, 2011). During the past decades, various technologies have been developed to prevent the attachment of bacteria to solid surfaces (Elius et al., 2023), including modification of surface properties (e.g., surface stiffness, surface roughness) (Francone, 2021; Hsu et al., 2013; Peng, 2019; Qi et al., 2017; Song et al., 2017), introduction of flow shear (Locsei and Pedley, 2009; Molaei and Sheng, 2016), and electric fields (Hong, 2008; Kang et al., 2011), and maintenance of a protective air layer over the solid body (Cai et al., 2021; Scardino et al., 2009). Among them, the bio-inspired super-hydrophobic surface (SHS), created by a combination of surface roughness and

hydrophobic chemistry, is one emerging technology for prevention of biofilm growth (Agabe et al., 2020; Chang, 2022; Dou et al., 2015; Iavanaugh, 2012, 2013; Jalil, 2020; Jiang, 2020; Pechook, 2015; Truong, 2012; Xiang, 2021; Zhang et al., 2020). Researchers have tested the antifouling properties of various types of SHS fabricated by methods including lithography (Francone, 2021; Houngkamhang, 2022; Lu et al., 2016), femtosecond/picosecond laser writing (Jalil, 2020; Sun, 2018), anodization (Bartlet et al., 2018), and chemical etching (Long et al., 2020). The attachment of bacteria on SHS has been quantified by various methods, such as fluorescent imaging (Siddique et al., 2020), confocal laser scanning microscopy (Bruzaud et al., 2017), and scanning electron microscopy (SEM) (Cuello et al., 2020). Most studies have shown that SHS could suppress the growth of biofilm, regardless of the type of surface roughness either in micro-scale (Cuello et al., 2020), or nano-scale (Bartlet et al., 2018; Bruzaud, 2017; Long, 2020), or a combination of both (Francone et al., 2021). The anti-biofouling efficiency of SHS was found to vary significantly, with a reduction in the number of

\* Corresponding author.

E-mail address: [hling1@umassd.edu](mailto:hling1@umassd.edu) (H. Ling).

attached bacteria ranging from 10% (Lu et al., 2016) to 99% (Jalil et al., 2020) compared to a smooth surface. Yet, it is still unclear what factors, such as SHS texture size, texture geometry, and surface chemistry, contribute to these variations.

Despite the extensive studies on the anti-biofouling properties of SHS, the mechanism of how SHS suppresses the biofilm growth is not well understood. In particular, the literature shows a disagreement with respect to the role of the micro/nano-scale gas bubbles trapped on the submerged SHS on the bacterial adhesion. Some studies (Chang, 2022; Ivanova, 2012; Mateescu et al., 2020) suggested that the trapped gas bubbles do not impact the bacterial adhesion and claimed that the surface roughness on SHS such as the sharp nanostructure is the origin of the low adhesion of bacteria to surface. In contrast, other studies by Truong et al. (2012) and Hwang et al. (2018) suggested that the trapped gas bubbles played an essential role on the anti-biofouling property of SHS. They reported that when the air layer on SHS is depleted (e.g., by gas diffusion), the SHS could adversely enhance the bacterial attachment due to the increase of surface roughness (Hwang et al., 2018).

In this study, we aim to study whether and how the gas bubbles trapped on the SHS impact the bacterial adhesion. In particular, we aim to test the hypothesis proposed by previous works (Hwang et al., 2018; Truong, 2012), that gas bubbles are essential for reducing bacterial adhesion. To achieve this goal, we performed novel experiments which measured the spatial distributions of gas bubbles, surface texture, and attached bacteria, and their relationships. If the gas bubbles prevented the bacterial adhesion, one would expect that the surface areas covered by the gas (i.e., areas between roughness element) is free of bacteria. SEM was selected as a proper tool in this study since it captured both the surface texture and the attached bacteria, and consequently allowed the examination of the correlation between gas bubbles and bacterial adhesion. The presence of gas bubbles on SHS was confirmed based on total-internal reflection and brightfield microscopy. Multiple surfaces were tested in this study including SHS with regular grooves, SHS with random micro/nano-scale roughness, and rough surfaces with the same texture geometry of the SHS. We will show that the surface areas covered by gas were free of bacteria, validating the hypothesis that the gas bubbles prevented the bacterial adhesion. In addition, we will show that the size of gas bubbles on SHS must be larger than the size of bacteria to effectively prevent bacterial adhesion. Our results provide a better understanding for the anti-biofouling mechanism of the SHS.

This work is different from previous works and is novel for following reasons. First, the spatial distributions of gas bubbles, surface texture, and attached bacterial were experimentally measured through techniques such as SEM and plastron visualization. Second, bacterial adhesion results on a range of surfaces, including surfaces with regular or random texture geometries, with or without hydrophobic chemistry, were compared. Due to these novelties, our work provided solid evidence to demonstrate the impact of gas bubbles on the bacterial adhesion on SHS.

## 2. Material and methods

### 2.1. Source of materials for SHS fabrication and testing

Aluminum plates, sandblasting media, and slitting saws were obtained from *McMaster Carr*. Hydrochloride acid (32%, CAS #7647-01-0), perfluoroctyltrioxysilane (98%, CAS #51851-37-7), hexane (95%, CAS #110-54-3), and Rhodamine B (>95%, CAS #81-88-9) were purchased from *Sigma-Aldrich*. Marine Broth (Catalog #DF0791-17-4) and Ethyl alcohol denatured (93%, CAS #64-17-5) were obtained from *Fisher Scientific*. Osmium tetroxide (2%, SKU #19152) and glutaraldehyde (2% in 0.1 M Sodium Cacodylate Buffer, SKU: 16536-15) were obtained from *Electron Microscopy Sciences*. Hexamethyldisilazane (98%, CAS # 999-97-3) was purchased from *Thermo Fisher Scientific*.

### 2.2. Fabrication of super-hydrophobic surfaces

The experimental procedure for testing the bacterial adhesion on SHS is shown in Fig. 1. First, we fabricated SHS on aluminum with two types of surface textures: one with regular micro-grooves, and the other with randomly roughed textures at micro/nano-scales. For the first surface texture type (grooved SHS), the micro-grooves were generated by a slitting saw, and had a period of 304 μm, a width of 152 μm, and a depth of 304 μm. These dimensions were selected such that the Cassie-Baxter state (Cassie and Baxter, 1944) is more thermodynamically favorable compared to the Wenzel state (Wenzel, 1936) as will be confirmed in the results. In Cassie-Baxter state, the liquid only contacts with the tip of the surface textures and the gas is trapped between the roughness elements. While in Wenzel state, the liquid fully wets the surface, and no gas is entrapped. Note, the purpose of this study is to confirm the impact of entrapped gas on the spatial distribution of bacterial adhesion, we didn't systematically vary the groove dimensions and study their impacts on the anti-biofouling efficiency of SHS.

For the second surface texture type (randomly roughed SHS), the surface roughness was created by sandblasting (the abrasive blasting media is a mixture of glass bead and aluminum oxide with grit size of 220), followed by chemical etching via 18 wt% hydrochloride solution for 90 s and boiling in hot water for 30 min. The sandblasting and chemical etching produce micro-scale texture with a size of 1–100 μm, while the boiling procedure generates nano-scale surface roughness with size of 10–100 nm (Kim et al., 2013). For both roughed surfaces, to functionalize them with hydrophobic chemistry, they were first cleaned ultrasonically with acetone and ethanol to get rid of grease, and then immersed in a solution of perfluoroctyltrioxysilane in hexane (7 μl/ml) for 24 h. Directly after immersing, the samples were baked in an oven at 120 °C for 1 h to ensure the chemical bonding of silane molecules to the surface. The chemical treatment procedure followed a method previously described in (Saranadhi et al., 2016).

### 2.3. Fabrication of rough surfaces

Two rough surfaces, one with the same texture geometry as the grooved SHS and one with the same texture geometry as the randomly roughed SHS, were also fabricated. We followed the same fabrication procedures described above to fabricate the surface roughness. These rough surfaces received no hydrophobic chemical treatment.

### 2.4. Visualization of gas bubbles on underwater surfaces

Following previous studies (Bobji et al., 2009; Mohammadshahi et al., 2023), we examined the presence of gas bubbles on underwater surfaces based on Total-Internal-Reflection (TIR). A CMOS camera (FLIR, model #GS3-U3-41C6M-C) and a LED light were used for the TIR imaging. The incident angle of light rays was 55°, greater than the critical angle (48°) for the occurrence of total internal reflection at water/air interface. The camera and light settings were kept the same for comparison between different surfaces or a same surface at different times. In the TIR images, the surface areas covered by the gas have much higher intensity compared to areas with no gas coverage.

For the grooved SHS, we further used brightfield microscopy to visualize the gas bubbles within the micro-grooves. The water was dyed by Rhodamine B at a concentration below 0.1 mg/mL to enhance the image contrast, the LED light illuminated the surface in a direction parallel to the grooves, and a color camera (FLIR, model #BFS-PGE-16S2C-CS) was used to capture the images.

### 2.5. Preparation of bacterial suspensions

The bacterial strain *Shewanella* sp. UMDC19, originally isolated from marine biofilms in Northwestern Atlantic Ocean was used in this study. For each experiment, the strain was aseptically inoculated from glycerol

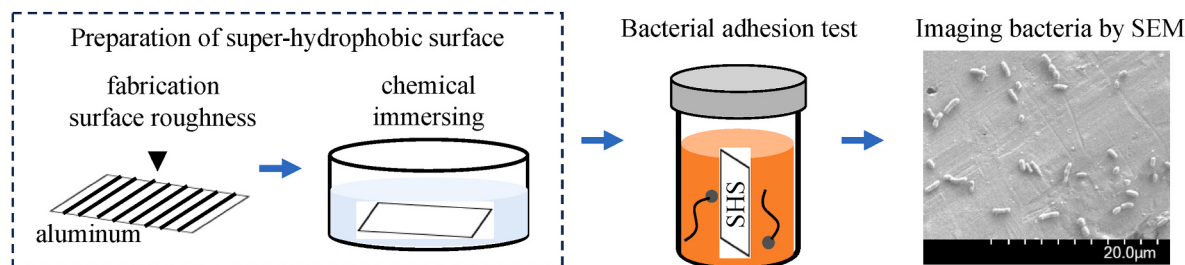


**Fig. 1.** A schematic drawing of experimental procedure for testing the bacterial adhesion on SHS.

stock and grown in sterile-filtered Marine Broth (SFMB) overnight at 27 °C in the dark in slow shaking motion.

#### 2.6. Bacterial adhesion to samples test

The 5 cm by 1 cm surfaces and an attached stainless steel wire were UV-sterilized for 20 min from both sides. A 5-mL snap-top tube with 3 mL SFMB was aseptically loop-inoculated with the overnight culture. The strip was immersed in the bacterial suspension and then kept in suspension without wall contact, by securing the wires with the lid. The tubes were then incubated for 20 h at 27 °C in the dark in slow motion. Optical density measurements showed that there was an equivalent level of bacterial growth in the tubes in the presence and absence of the surfaces.

#### 2.7. Imaging attached bacteria by scanning electron microscopy

The sample preparation for SEM imaging was modified from the method described in (Schu et al., 2021). Immediately after the bacterial adhesion tests, the surfaces were removed to a new tube and bacteria were fixed by adding 3 mL 2% glutaraldehyde in 0.1M sodium cacodylate. Each of the subsequent steps was conducted by first removing the liquid from the prior step and then adding the new solution. After fixation (1–18 h), the surfaces were treated with 3 mL of 0.2 M sodium cacodylate buffer three times for 10 min. Three mL 1% osmium tetroxide

was then added and tubes kept at room temperature for 1 h. The surfaces were then rinsed with 3 mL of Reverse Osmosis water (RO) three times for 5 min per wash. Samples were then dehydrated with a series of 50% (5 min), 70% (5 min), 95% (10 min) and 100% (10 min) EtOH (3 mL each). The samples were then chemically dried using a hexamethyldisilazane (HMDS) series. Samples were first treated with 3 mL of HMDS: EtOH at 1:2, then 2:1 (vol:vol) for 15 min each, followed by two 100% HMDS treatments for 15 min each. The samples were dried overnight, then kept in a desiccator in room temperature. The surfaces were attached to SEM stubs using carbon tape, then gold or gold + palladium sputter-coated. The spatial distribution of attached bacteria on SHS was studied by a field emission Scanning Electron Microscope (Hitachi SU-5000). A voltage of 2.5–3.5 KV was used for SEM imaging.

Noted that our goal in this study is to examine the relationship between trapped gas bubbles on textured SHS and bacterial adhesion, rather than to quantify the anti-biofouling efficiency or develop a better anti-biofouling material. Therefore, we believe that SEM imaging is sufficient for our study to examine which surface areas are impacted by bacteria after the bacterial adhesion test. We did not stain the bacteria and used fluorescent microscopy to quantify the number of attached bacteria as typically did by other researchers.

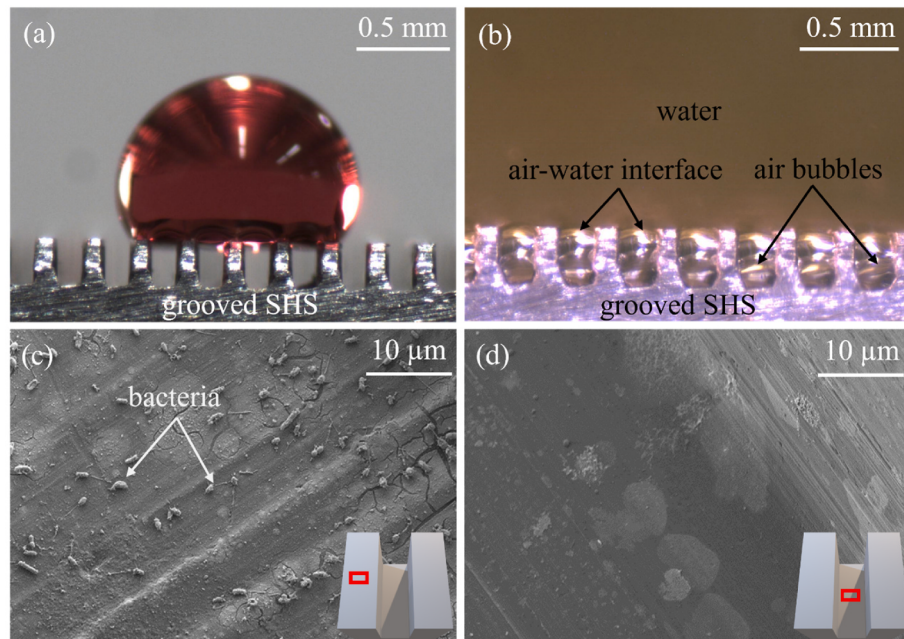


**Fig. 2.** Experimental results on the grooved super-hydrophobic surface: (a) a water droplet seating on the surface showing the Cassie Baxter state; (b) presence of gas bubbles within the micro-grooves when the surface is fully immersed in water; (c-d) SEM images of the top of ridge (c) and bottom of the groove (d) after the bacterial adhesion test. More SEM images for this sample can be found at Supplementary fig. S1.

### 3. Results and discussion

#### 3.1. A. bacterial adhesion on super-hydrophobic surfaces

First, we show experimental results on the grooved SHS. As shown in Fig. 2a, the grooved SHS promoted a Cassie-Baxter state where the water droplet was seated only on the top of surface roughness. When fully immersed in water, the SHS trapped a layer of gas bubbles within the grooves (Fig. 2b). Note, although the grooved SHS has a water contact angle less than  $150^\circ$ , we considered this sample as a super-hydrophobic surface for the reason that it had the same property as SHS: promoting Cassie-Baxter state and trapping gas bubbles when submerged underwater. After the bacterial adhesion test, we found that bacteria only attached to the top of surface roughness (area not covered by gas) (Fig. 2c; Supplementary fig. S1), not the bottom of the grooves (area covered by the gas bubbles) (Fig. 2d; Supplementary fig. S1). This result confirms that the gas bubbles on SHS act as a physical barrier that prevents bacteria from reaching the solid surface and thus protect the solid surface from bacterial adhesion. This result agrees with previous studies which showed the important role of the gas on the anti-biofouling performance of SHS (Hwang et al., 2018; Truong, 2012).

Second, we show experimental results on the randomly roughed SHS with micro/nano-scale textures. As shown in Fig. 3a, the surface had a high water contact angle of  $152^\circ$ . The measured sliding angle was less than  $5^\circ$ . The high intensity presence on the TIR image, as shown in Fig. 3b, indicates the presence of gas bubbles within the surface roughness. It should be noted that due to the multi-length scale of the surface texture, both micro-scale and nano-scale gas bubbles were trapped on the surface. After the bacterial adhesion test, we found that between the micro-scale roughness elements which were covered by micro-scale gas bubbles, there were no attached bacteria (Fig. 3c; Supplementary fig. S2). This result is consistent with the observation on grooved SHS, again validating that the micro-scale gas bubbles protect

the solid surface from bacterial adhesion.

However, we found bacteria attached to the top of micro-scale roughness elements (Fig. 3c; Supplementary fig. S2), even though these locations had nanoscale roughness. We also fabricated nano-scale surface roughness on the grooved SHS by applying an additional boiling procedure (same procedure for producing nano-scale roughness on the randomly roughed SHS) before the hydrophobic chemical treatment, and performed bacterial adhesion test. We found the same result showing that bacteria were present on the top of micro-ridges although

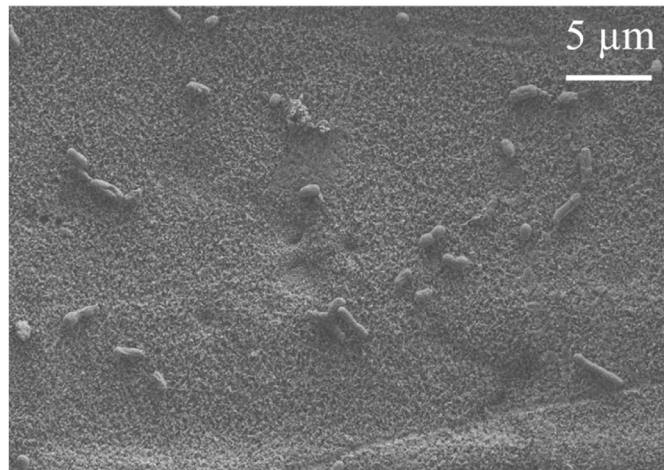


**Fig. 4.** SEM image showing the presence of adhesive bacteria on SHS at a location covered by nano-scale roughness. The SHS was created by following the same procedure as that of the grooved SHS but with an additional boiling process before the hydrophobic chemical treatment. The surface area shown in the SEM image is at the top of micro-ridges.

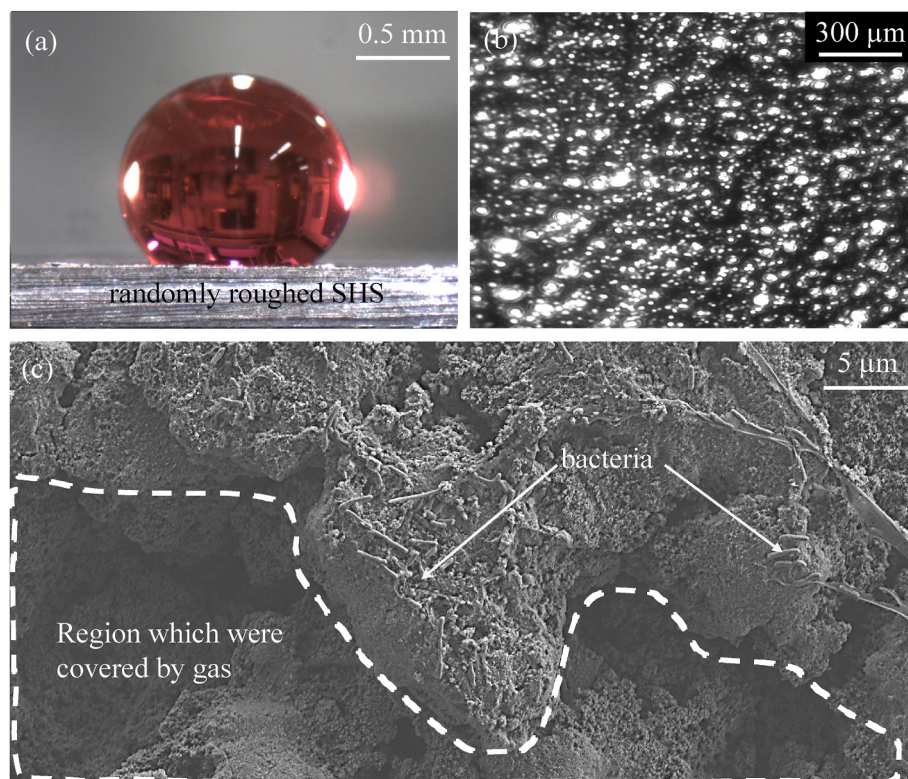


**Fig. 3.** Experimental results on the randomly-roughed super-hydrophobic surface: (a) a water droplet seating on the surface; (b) TIR image showing the presence of gas bubbles on the surface; (c) SEM image of the surface after the bacterial adhesion test showing bacteria attached only to the tops, not gaps of roughness elements. More SEM images for this sample can be found at Supplementary fig. S2.

these locations are covered by nano-scale roughness (Fig. 4). There are two possible reasons for this observation. First, the gas trapped between the nano-scale roughness may be dissolved into the liquid. At the end of the experiments, there might be no gas trapped between the nano-scale roughness. Note, at the beginning of the experiment, there must be gas trapped between the nano-scale roughness. As shown in Supplementary fig. S3, a surface with nano-scale roughness had a high water contact angle, indicating the presence of gas within the nano-scale roughness. However, due to the small size, we were unable to directly measure the nano-scale gas bubbles and validate the presence of nano-scale gas on the surface. Second, even though the gas may be trapped between the nano-roughness throughout the experiment, these nano-scale gas bubbles may not be effective in preventing bacterial adhesion. It may be that when the body size of bacteria (2–3  $\mu\text{m}$  in length) is larger than the entrapped nano-scale gas bubbles (size 10–100 nm), bacteria are still able to find contact points with the solid surface and adhere to the surface. It should be noted that although nano-scale roughness may not directly prevent bacterial adhesion, they could enhance the stability of micro-scale gas bubbles against pressure (Xue et al., 2012) and turbulent flows (Heo et al., 2021).

### 3.2. B. longevity of gas on super-hydrophobic surfaces

The gas on SHS could diffuse into ambient liquid at a rate increasing with the immersing depth of the sample in the liquid (Poetes et al., 2010) and the under-saturation level of the surrounding liquid (Nosrati et al., 2023). To test if the gas bubbles remained on the SHSs during the entire 20 h bacterial adhesion tests, we performed separate experiments by immersing our fabricated SHSs in DI water at a depth of 5 cm (the same depth as the bacterial adhesion tests) and measuring the gas layer on SHS based on TIR. Before the tests, the water was exposed to air at atmosphere pressure for more than 2 days such that it was saturated with air at atmosphere pressure. Fig. 5(a) and (b) show that the gas bubbles remained on both grooved SHS and randomly roughed SHS after immersing in water for 20 h. A theoretical prediction based on a model proposed in (Bourgoun and Ling, 2022) also suggested that the longevity of gas bubbles under current experimental condition was longer than 20 h (see Supplementary Material). Note, the current experiments were performed under an ideal condition, the longevity of gas on SHS may be much shorter in real applications due to a higher under-saturation level of the surrounding liquid (Nosrati et al., 2023) and turbulent flows (Ling et al., 2017; Mohammadshahi et al., 2024).

It should also be noted that Fig. 5b only confirms the existence of micro-scale gas trapped between the micro-scale roughness. Due to the limited spatial resolution, the imaging method used in this study was unable to validate the existence of nano-scale gas trapped between the nano-scale roughness.

### 3.3. C. bacterial adhesion on rough surfaces

Finally, to confirm that the non-uniform distributions of bacteria were indeed caused by gas bubbles not due to the surface roughness itself, we performed bacterial adhesion tests for surfaces having the same texture geometry as the SHSs but ones that did not have the hydrophobic coating. These control surfaces did not trap any gas bubbles when immersed in liquid. The reason that no gas bubbles were trapped was because these rough surfaces were made from aluminum and were hydrophilic. Thus, the Wenzel state was more thermodynamically favorable compared to the Cassie-Baxter state.

Fig. 6 shows the results for the grooved surface, and Fig. 7 shows the results for the randomly roughed surface, each with similar surface geometry as the SHS equivalent, but not containing the hydrophobic chemical treatment. As expected, with no hydrophobic coating, these rough surfaces promoted a Wenzel state where the water droplet fully wetted the surfaces (Fig. 6a) and had a smaller water contact angle than the SHS counterpart (Fig. 7a). When submerged in water, no gas bubbles were trapped within the surface roughness (Figs. 6b and 7b). After the bacterial adhesion test, bacteria were found throughout these rough surfaces, including both the top and bottom of the roughness elements (Fig. 6c–d, 7c, Supplementary figs. S4 and S5). Therefore, we confirmed that the surface roughness alone as used in this study did not alter the spatial distributions of bacteria.

Although some studies (Qi et al.) showed that surface hydrophobicity also played an important role for the adhesion of bacteria, we found that the impact of surface hydrophobicity was minor in our experiments. First, comparing Fig. 2(c) and (d), although the surface hydrophobic was same (since the entire surface was uniformly coated by perfluoroctyltriethoxysilane), the numbers of adhered bacterial were different. As explained earlier, this difference was due to the presence of gas bubble between the roughness elements. Second, as shown in Figs. 2(c) and 6(c), at the top of roughness elements, although one surface was hydrophobic and the other was hydrophilic, the numbers of adhered bacterial were similar.

In summary, our study showed that SHS altered the spatial distribution of bacteria: bacteria only attached to surface area that were not covered by gas, while a rough surface with the same texture geometry of SHS did not change the bacteria distribution. It should be noted that the SEM results shown in Figs. 2 and 3 did not necessarily mean the fabricated SHS reduce the overall bacteria adhesion. To quantify the anti-fouling properties of the fabricated samples, more statistical results are needed. Yet, our result suggests that the anti-fouling properties of SHS observed in previous studies could attribute to the presence of gas on the surface. However, since our study only considered two types of SHS, more studies are required to test if our conclusion could apply to SHS with different texture sizes, gas fractions and texture geometries (e.g., regular posts, holes). In particular, for a SHS with a sharp texture which has the capability to kill bacteria, the results might be different. More studies are also needed to determine the optimal SHS texture for

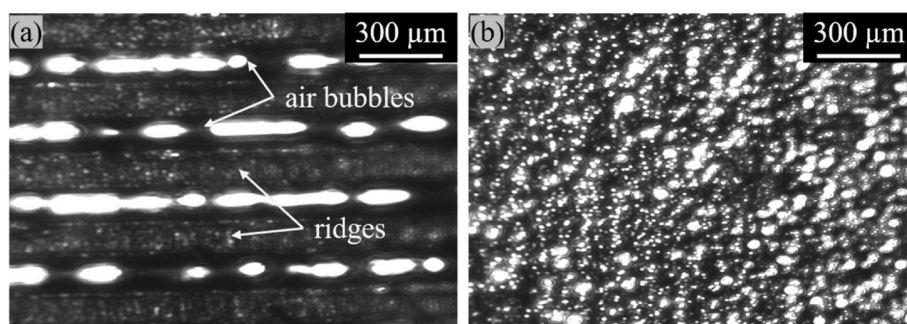


**Fig. 5.** Status of the gas layer on grooved SHS (a) and randomly roughed SHS (b) after immersing in DI water at a depth of 5 cm for 20 h. The images were obtained based on Total-Internal Reflection.

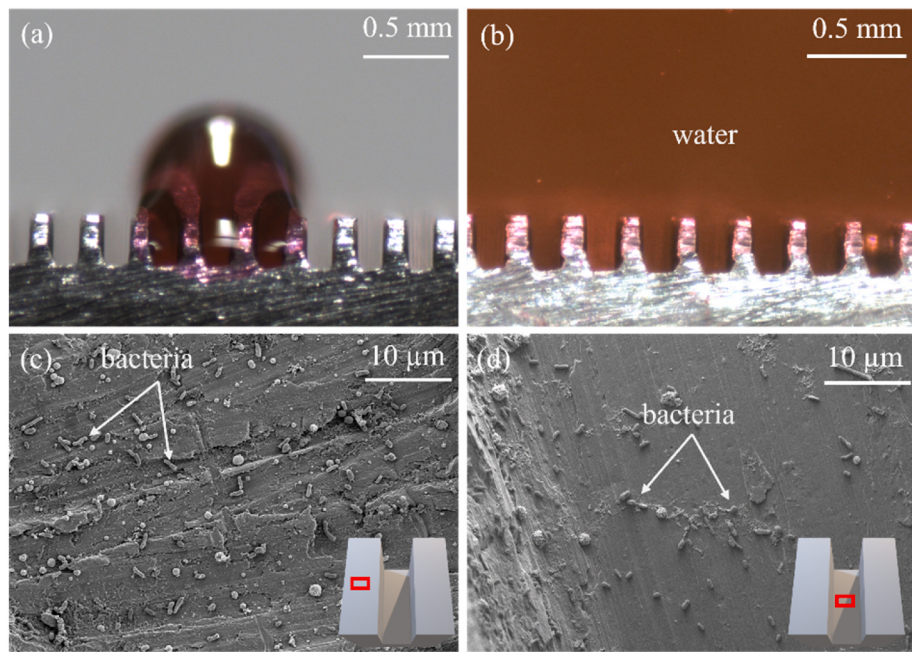


**Fig. 6.** Experimental results on the grooved surface with no hydrophobic coating: (a) a water droplet seating on the surface showing the Wenzel state; (b) no gas bubbles present when the surface is fully immersed in water; (c–d) SEM images of the top of ridge (c) and bottom of the groove (d) after the bacterial adhesion test. More SEM images for this sample can be found at Supplementary fig. S3.

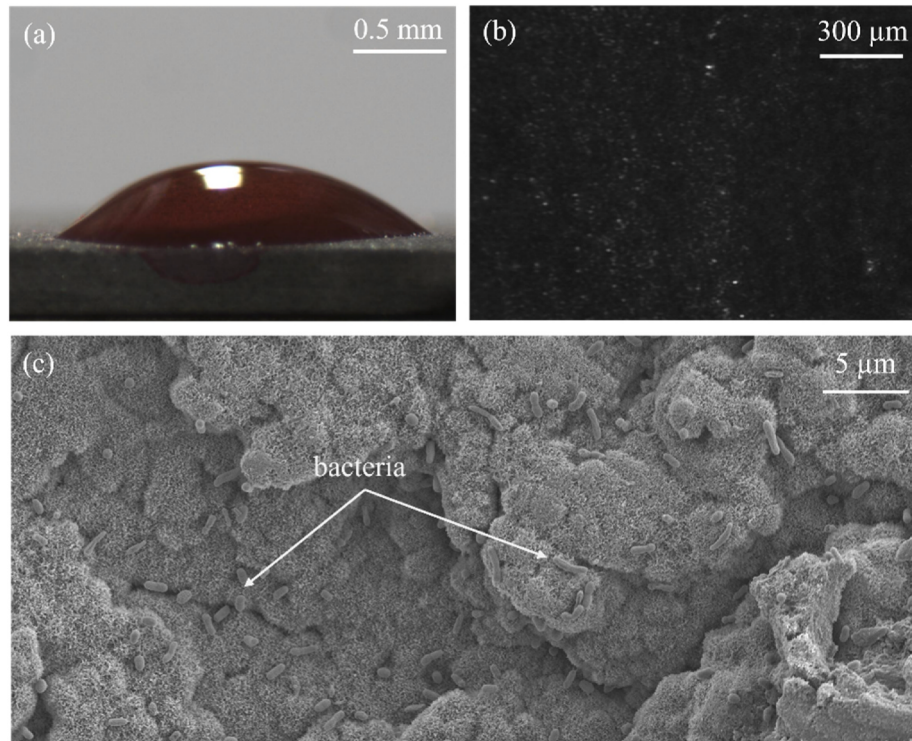


**Fig. 7.** Experimental results on the randomly roughed surface with no hydrophobic coating: (a) a water droplet seating on the surface showing low contact angle; (b) TIR image showing no gas bubbles attached to the surface; (c) SEM image of the surface after the bacterial adhesion test showing bacteria attached at both gaps and tops of roughness elements. More SEM images for this sample can be found at Supplementary fig. S4.

reducing bacteria adhesion and maintaining a stable Cassie-Baxter state.

#### 4. Conclusions

In summary, we studied how the micro/nano-gas bubbles trapped on

the SHS influent the spatial distribution of bacterial attachment by using scanning electron microscopy. We found that the surface areas covered by micro-scale gas bubbles promoted by gaps between roughness elements were free of bacteria, while surface areas exposed to liquid allowed bacterial adhesion. Our results suggest that the anti-biofouling

properties of SHS found in previous works could attribute to the physical barrier of gas-liquid interface which separates bacteria from the solid walls. Furthermore, we found that bacteria were able to attach to surface areas covered by nano-scale surface roughness. More controlled experiments are needed to understand whether the reason was due to the dissolution of nano-scale gas or the small size of the nano-scale gas. More experiments are needed to study the effect of gas bubble size on the bacterial attachment, and to demonstrate whether the gas bubbles must be larger than the bacterial cell size to achieve anti-bacterial performance. We believe these results can guide the design of more efficient anti-biofouling materials. For example, our results suggest that SHS with a larger percentage of surface area covered by gas (or gas fraction) should have a higher anti-biofouling efficiency. Future studies are required to test this hypothesis. Future studies are also required to validate the anti-bacterial performance of similar SHS under flow conditions.

The duration of our bacteria adhesion test was 20 h. We believe this duration was sufficient for current investigation of the influence of gas bubbles on the SHS on bacteria adhesion. However, for general application such as marine anti-biofouling, the adhesion of bacteria is the early stage of biofouling process. After a few days, large organisms such as larvae or spores may adhere to the surface. Experiments with longer durations are required to test whether the gas bubbles on the SHS could effectively protect the surface from these large organisms.

## Funding

UMass Dartmouth's Marine and Undersea Technology (MUST) Research Program funded by the Office of Naval Research (ONR) under Grant No. N00014-20-1-2170. The Office of Technology Commercialization & Ventures (OTCV) Technology Development Fund from University of Massachusetts's President's Office.

## CRediT authorship contribution statement

**Md Elius:** Writing – original draft, Methodology, Investigation, Formal analysis, Data curation. **Stephanie Richard:** Writing – original draft, Methodology, Data curation. **Kenneth Boyle:** Writing – original draft, Methodology, Data curation. **Wei-Shun Chang:** Supervision, Funding acquisition, Conceptualization. **Pia H. Moisander:** Supervision, Funding acquisition, Conceptualization. **Hangjian Ling:** Writing – review & editing, Writing – original draft, Supervision, Funding acquisition, Conceptualization.

## Declaration of competing interest

The authors declare that they have no known competing financial interests or personal relationships that could have appeared to influence the work reported in this paper.

## Data availability

Data will be made available on request.

## Acknowledgement

We thank Paul Sousa for assistance in the grooved surface fabrication.

## Appendix A. Supplementary data

Supplementary data to this article can be found online at <https://doi.org/10.1016/j.surfin.2024.100211>.

## References

- Agbe, H., Sarkar, D.K., Chen, X.-G., 2020. Tunable superhydrophobic aluminum surfaces with anti-biofouling and antibacterial properties. *Coatings* 10 (10). <https://doi.org/10.3390/coatings10100982>. Art. no. 10.
- Bartlet, K., Movafaghi, S., Dasi, L.P., Kota, A.K., Popat, K.C., 2018. Antibacterial activity on superhydrophobic titania nanotube arrays. *Colloids Surf. B Biointerfaces* 166, 179–186. <https://doi.org/10.1016/j.colsurfb.2018.03.019>.
- Bobji, M.S., Kumar, S.V., Asthana, A., Govardhan, R.N., 2009. Underwater Sustainability of the 'Cassie' state of wetting. *Langmuir* 25 (20), 12120–12126. <https://doi.org/10.1021/la902679c>.
- Bourgoin, A., Ling, H., 2022. A general model for the longevity of super-hydrophobic surfaces in under-saturated, stationary liquid. *J. Heat Tran.* 144 (4) <https://doi.org/10.1115/1.4053678>.
- Bruzaud, J., et al., 2017. The design of superhydrophobic stainless steel surfaces by controlling nanostructures: a key parameter to reduce the implantation of pathogenic bacteria. *Mater. Sci. Eng. C* 73, 40–47. <https://doi.org/10.1016/j.msec.2016.11.115>.
- Cai, Y., Bing, W., Chen, C., Chen, Z., 2021. Gaseous plastron on Natural and biomimetic surfaces for resisting marine biofouling. *Molecules* 26 (9). <https://doi.org/10.3390/molecules26092592>, 9.
- Callow, M., Callow, J.E., 2002. *Marine Biofouling: a Sticky Problem*. Biologist.
- Cassie, A.B.D., Baxter, S., 1944. Wettability of porous surfaces. *Trans. Faraday Soc.* 40 (O), 546–551. <https://doi.org/10.1039/TF9444000546>.
- Chang, X., et al., 2022. Superhydrophobic micro-nano structured PTFE/WO<sub>3</sub> coating on low-temperature steel with outstanding anti-pollution, anti-icing, and anti-fouling performance. *Surf. Coatings Technol.* 434, 128214 <https://doi.org/10.1016/j.surcoat.2022.128214>.
- Costerton, J.W., Lewandowski, Z., Caldwell, D.E., Korber, D.R., Lappin-Scott, H.M., 1995. Microbial biofilms. *Annu. Rev. Microbiol.* 49, 711–747.
- Cuello, E.A., Mulko, L.E., Barbero, C.A., Acevedo, D.F., Yslas, E.I., 2020. Development of micropatterning polyimide films for enhanced antifouling and antibacterial properties. *Colloids Surf. B Biointerfaces* 188, 110801. <https://doi.org/10.1016/j.colsurfb.2020.110801>.
- Dou, X.-Q., Zhang, D., Feng, C., Jiang, L., 2015. Bioinspired Hierarchical Surface Structures with Tunable Wettability for Regulating Bacteria Adhesion. *ACS Nano* 9 (11), 10664–10672. <https://doi.org/10.1021/acsnano.5b04231>.
- Elius, M., Boyle, K., Chang, W., Moisander, P., Ling, H., 2023. Comparison of three-dimensional motion of bacteria with and without wall accumulation. *Phys. Rev. E* 108 (1), 014409 <https://doi.org/10.1103/PhysRevE.108.011409>.
- Fitridge, I., Dempster, T., Guenther, J., de Nys, R., 2012. The impact and control of biofouling in marine aquaculture: a review. *Biofouling* 28 (7), 649–669. <https://doi.org/10.1080/08927014.2012.700478>.
- Francone, A., et al., 2021. Impact of surface topography on the bacterial attachment to micro- and nano-patterned polymer films. *Surface. Interfac.* 27, 101494 <https://doi.org/10.1016/j.surfin.2021.101494>.
- Habash, M., Reid, G., 1999. Microbial biofilms: their development and significance for medical device-related infections. *J. Clin. Pharmacol.* 39 (9), 887–898. <https://doi.org/10.1177/00912709922008506>.
- Hong, S.H., et al., 2008. Effect of electric currents on bacterial detachment and inactivation. *Biotechnol. Bioeng.* 100 (2), 379–386. <https://doi.org/10.1002/bit.21760>.
- Houngkamhang, N., et al., 2022. Enhancement of bacterial anti-adhesion properties on robust PDMS micro-structure using a simple flame treatment method. *Nanomaterials* 12 (3). <https://doi.org/10.3390/nano12030557>. Art. no. 3.
- Hsu, L.C., Fang, J., Borca-Tasciuc, D.A., Worobo, R.W., Moraru, C.I., 2013. Effect of micro- and nanoscale topography on the adhesion of bacterial cells to solid surfaces. *Appl. Environ. Microbiol.* 79 (8), 2703–2712. <https://doi.org/10.1128/AEM.03436-12>.
- Hwang, G.B., Page, K., Patir, A., Nair, S.P., Allan, E., Parkin, I.P., 2018. The anti-biofouling properties of superhydrophobic surfaces are short-lived. *ACS Nano* 12 (6), 6050–6058. <https://doi.org/10.1021/acsnano.8b02293>.
- Ivanova, E.P., et al., 2013. Bactericidal activity of black silicon. *Nat. Commun.* 4 (1) <https://doi.org/10.1038/ncomms3838>. Art. no. 1.
- Ivanova, E.P., et al., 2012. Natural bactericidal surfaces: mechanical rupture of *Pseudomonas aeruginosa* cells by cicada wings. *Small* 8 (16), 2489–2494. <https://doi.org/10.1002/smll.201200528>.
- Jalil, S.A., et al., 2020. Creating superhydrophobic and antibacterial surfaces on gold by femtosecond laser pulses. *Appl. Surf. Sci.* 506, 144952 <https://doi.org/10.1016/j.apsusc.2019.144952>.
- Jiang, R., et al., 2020. Lotus-leaf-inspired hierarchical structured surface with non-fouling and mechanical bactericidal performances. *Chem. Eng. J.* 398, 125609 <https://doi.org/10.1016/j.cej.2020.125609>.
- Kang, H., Shim, S., Lee, S.J., Yoon, J., Ahn, K.H., 2011. Bacterial translational motion on the electrode surface under anodic electric field. *Environ. Sci. Technol.* 45 (13), 5769–5774. <https://doi.org/10.1021/es200752h>.
- Kim, P., Kreder, M.J., Alvarenga, J., Aizenberg, J., 2013. Hierarchical or not? Effect of the length scale and hierarchy of the surface roughness on omniphobicity of lubricant-infused substrates. *Nano Lett.* 13 (4), 1793–1799. <https://doi.org/10.1021/nl4003969>.
- Ling, H., Katz, J., Fu, M., Hultmark, M., 2017. Effect of Reynolds number and saturation level on gas diffusion in and out of a superhydrophobic surface. *Phys. Rev. Fluids* 2 (12), 124005. <https://doi.org/10.1103/PhysRevFluids.2.124005>.
- Locsei, J.T., Pedley, T.J., 2009. Run and tumble chemotaxis in a shear flow: the effect of temporal comparisons, persistence, rotational diffusion, and cell shape. *Bull. Math. Biol.* 71 (5), 1089–1116. <https://doi.org/10.1007/s11538-009-9395-9>.

- Long, W., et al., 2020. Superhydrophobic diamond-coated Si nanowires for application of anti-biofouling. *J. Mater. Sci. Technol.* 48, 1–8. <https://doi.org/10.1016/j.jmst.2019.10.040>.
- Lu, N., Zhang, W., Weng, Y., Chen, X., Cheng, Y., Zhou, P., 2016. Fabrication of PDMS surfaces with micro patterns and the effect of pattern sizes on bacteria adhesion. *Food Control* 68, 344–351. <https://doi.org/10.1016/j.foodcont.2016.04.014>.
- Mateescu, M., Knopf, S., Mermet, F., Lavalle, P., Vonna, L., 2020. Role of trapped air in the attachment of *Staphylococcus aureus* on superhydrophobic silicone elastomer surfaces textured by a femtosecond laser. *Langmuir* 36 (5), 1103–1112. <https://doi.org/10.1021/acs.langmuir.9b03170>.
- Mihai, M.M., et al., 2015. Microbial biofilms: impact on the pathogenesis of periodontitis, cystic fibrosis, chronic wounds and medical device-related infections. *Curr. Top. Med. Chem.* 15 (16), 1552–1576. <https://doi.org/10.2174/15680266150414123800>.
- Mohammadshahi, S., Breveleri, J., Ling, H., 2023. Fabrication and characterization of super-hydrophobic surfaces based on sandpapers and nano-particle coatings. *Colloids and Surf. A Physicochem. Eng. Asp.* 666, 131358. <https://doi.org/10.1016/j.colsurfa.2023.131358>.
- Mohammadshahi, S., O'Cain, D., Ling, H., 2024. Impact of sandpaper grit size on drag reduction and plastron stability of super-hydrophobic surface in turbulent flows. *Physcis of Fluids* 36 (2), 025139. <https://doi.org/10.1063/5.0187081>.
- Molaei, M., Sheng, J., 2016. Succeed escape: flow shear promotes tumbling of *Escherichia coli* on a solid surface. *Sci. Rep.* 6 (1) <https://doi.org/10.1038/srep35290>. Art. no. 1.
- Myszka, K., Czaczik, K., 2011. Bacterial biofilms on food contact surfaces - a review. *Pol. J. Food Nutr. Sci.* 61 (3), 173–180. <https://doi.org/10.2478/v10222-011-0018-4>.
- Nosrati, A., Mohammadshahi, S., Raessi, M., Ling, H., 2023. Impact of the undersaturation level on the longevity of superhydrophobic surfaces in stationary liquids. *Langmuir* 39 (49), 18124–18131. <https://doi.org/10.1021/acs.langmuir.3c03006>.
- Pechook, S., et al., 2015. Bioinspired passive anti-biofouling surfaces preventing biofilm formation. *J. Mater. Chem. B* 3 (7), 1371–1378. <https://doi.org/10.1039/C4TB01522C>.
- Peng, Q., et al., 2019. Three-dimensional bacterial motions near a surface investigated by digital holographic microscopy: effect of surface stiffness. *Langmuir* 35 (37), 12257–12263. <https://doi.org/10.1021/acs.langmuir.9b02103>.
- Poetes, R., Holtzmann, K., Franze, K., Steiner, U., 2010. Metastable underwater superhydrophobicity. *Phys. Rev. Lett.* 105 (16), 166104 <https://doi.org/10.1103/PhysRevLett.105.166104>.
- Qi, M., Gong, X., Wu, B., Zhang, G., 2017. Landing dynamics of swimming bacteria on a polymeric surface: effect of surface properties. *Langmuir* 33 (14), 3525–3533. <https://doi.org/10.1021/acs.langmuir.7b00439>.
- Saranadhi, D., Chen, D., Kleingartner, J.A., Srinivasan, S., Cohen, R.E., McKinley, G.H., 2016. Sustained drag reduction in a turbulent flow using a low-temperature Leidenfrost surface. *Sci. Adv.* 2 (10) <https://doi.org/10.1126/sciadv.1600686>, 1600686.
- Scardino, A.J., Fletcher, L.E., Lewis, J.A., 2009. Fouling control using air bubble curtains: protection for stationary vessels. *Journal of Marine Engineering & Technology* 8 (1), 3–10. <https://doi.org/10.1080/20464177.2009.11020214>.
- Schu, M., Terriac, E., Koch, M., Paschke, S., Lautenschläger, F., Flormann, D.A.D., 2021. Scanning electron microscopy preparation of the cellular actin cortex: a quantitative comparison between critical point drying and hexamethyldisilazane drying. *PLoS One* 16 (7). <https://doi.org/10.1371/journal.pone.0254165>, 0254165.
- Siddique, R.Y., Gaddam, A., Agrawal, A., Dimov, S.S., Joshi, S.S., 2020. Anti-biofouling properties of femtosecond laser-induced submicron topographies on elastomeric surfaces. *Langmuir* 36 (19), 5349–5358. <https://doi.org/10.1021/acs.langmuir.0c00753>.
- Song, F., Brasch, M.E., Wang, H., Henderson, J.H., Sauer, K., Ren, D., 2017. How bacteria respond to material stiffness during attachment: a role of *Escherichia coli* flagellar motility. *ACS Appl. Mater. Interfaces* 9 (27), 22176. <https://doi.org/10.1021/acsami.7b04757>, –22184.
- Sun, K., et al., 2018. Anti-biofouling superhydrophobic surface fabricated by picosecond laser texturing of stainless steel. *Appl. Surf. Sci.* 436, 263–267. <https://doi.org/10.1016/j.apsusc.2017.12.012>.
- S, 허성광, Heo, W., 최우록, Choi, S. J., 이상준, Lee, 2021. Enhanced air stability of ridged superhydrophobic surface with nanostructure. *AIP Adv.* 11 (10), 105209 <https://doi.org/10.1063/5.0067279>.
- Truong, V.K., et al., 2012. Air-directed attachment of coccoid bacteria to the surface of superhydrophobic lotus-like titanium. *Biofouling* 28 (6), 539–550. <https://doi.org/10.1080/08927014.2012.694426>.
- Wenzel, R.N., 1936. Resistance of solid surfaces to wetting by water. *Ind. Eng. Chem.* 28 (8), 988–994. <https://doi.org/10.1021/ie50320a024>.
- Xiang, Y., et al., 2021. Superhydrophobic LDH/TTOS composite surface based on microstructure for the anti-corrosion, anti-fouling and oil-water separation application. *Colloids Surf. A Physicochem. Eng. Asp.* 622, 126558 <https://doi.org/10.1016/j.colsurfa.2021.126558>.
- Xue, Y., Chu, S., Lv, P., Duan, H., 2012. Importance of hierarchical structures in wetting stability on submersed superhydrophobic surfaces. *Langmuir* 28 (25), 9440–9450. <https://doi.org/10.1021/la300331e>.
- Zhang, J., Wang, J., Zhang, B., Zeng, Y., Duan, J., Hou, B., 2020. Fabrication of anodized superhydrophobic 5083 aluminum alloy surface for marine anti-corrosion and anti-biofouling. *J. Ocean. Limnol.* 38 (4), 1246–1255. <https://doi.org/10.1007/s00343-020-0036-3>.